Protein Science (1994), *3*:467–475. Cambridge University Press. Printed in the USA.

Mutational and crystallographic analyses of the active site residues of the *Bacillus circulans* xylanase

WARREN W. WAKARCHUK, ROBERT L. CAMPBELL, WING L. SUNG, JAMSHID DAVOODI, AND MAKOTO YAGUCHI

Institute for Biological Sciences, National Research Council of Canada, Ottawa, Ontario K1A 0R6, Canada

(RECEIVED October 26, 1993; ACCEPTED December 16, 1993)

Abstract

Using site-directed mutagenesis we have investigated the catalytic residues in a xylanase from *Bacillus circulans*. Analysis of the mutants E78D and E172D indicated that mutations in these conserved residues do not grossly alter the structure of the enzyme and that these residues participate in the catalytic mechanism. We have now determined the crystal structure of an enzyme–substrate complex to 1.8 Å resolution using a catalytically incompetent mutant (E172C). In addition to the catalytic residues, Glu 78 and Glu 172, we have identified 2 tyrosine residues, Tyr 69 and Tyr 80, which likely function in substrate binding, and an arginine residue, Arg 112, which plays an important role in the active site of this enzyme. On the basis of our work we would propose that Glu 78 is the nucleophile and that Glu 172 is the acid–base catalyst in the reaction.

Keywords: catalytic residues; enzyme mechanism; enzyme–substrate complex; nucleophile; xylanase

Glycosidases use a reaction mechanism based on acid catalysis by acidic amino acid residues (Sinnott, 1990). These residues have been identified and probed by X-ray crystallography, protein chemistry, enzymology, and site-directed mutagenesis to determine their roles in catalysis (Phillips, 1967; Rouvinen et al., 1990; Chauvaux et al., 1992; Juy et al., 1992; Mooser, 1992; Davies et al., 1993). These techniques are now being applied to cellulases and xylanases, which already have commercial applications (Yang et al., 1992; Gilbert & Hazlewood, 1993; Sung et al., 1993). As part of the growing interest in protein engineering of enzymes, which can be exploited in industrial processes, endo-β-1,4-D-xylanases (EC 3.2.1.8) have been found to be an effective biochemical means of decreasing the amount of chemical agents required to bleach pulp used in paper production (Viikari et al., 1986; Paice et al., 1992).

We have examined the properties of the *Bacillus circulans* 20-kDa xylanase, which is a member of family G xylanases according to the glycosidase classification scheme of Gilkes et al. (1991), with the goal of engineering it for wider application in the pulp and paper industry. The catalytic mechanism of this enzyme has been probed to understand its substrate specificity and the contributions that specific residues make in determining the activity of this class of enzyme.

Chemical modification studies with another family G xylanase, the *Schizophyllum commune* xylanase (*xyn*A), indicated that acidic residues were involved in catalysis (Bray & Clarke, 1990). These investigators showed the pK_a value for one of these residues was elevated and suggested that the residue was an acid catalyst similar to Glu 35 of hen egg white lysozyme (HEWL). An investigation of the stereochemical course of the reaction with *B. circulans* and *S. commune* xylanases indicated that the reaction proceeds with retention of configuration at the anomeric center (Gebler et al., 1992). The *B. circulans* xylanase also catalyzes transglycosylation (Wakarchuk, unpubl.). These results indicated that the enzyme mechanism is one of general acid catalysis using a nucleophile (or charge-stabilizing residue) and an acid–base catalyst similar to the mechanism of other glycosidases that show retention of the substrate's anomeric configuration in their products (Fig. 1; Sinnott, 1990; Kempton & Withers, 1992; Mooser, 1992). An analysis of a primary sequence alignment of 15 family G xylanases indicated that only 2 glutamic acid residues were absolutely conserved in this family of xylanases (Fig. 2). We, as well as others, have published preliminary data about mutations at these glutamic acid residues (Katsube et al., 1990; Wakarchuk et al., 1992), and we have proposed that Glu 78 and Glu 172 are the catalytic residues. A recent report from Ko et al. (1992) showed that 2 glutamic acid residues were involved in the catalytic mechanism of the *Bacillus pumilus* family G xylanase.

Our mutational analysis has been combined with an X-ray crystallographic structure of an enzyme–substrate complex to provide a more detailed description of the active site and the mechanism of action for this enzyme. We show here that the 2 glutamic acid residues Glu 78 and Glu 172 are intimately involved in catalysis, that Arg 112 also plays a role in cataly-

Reprint requests to: Warren W. Wakarchuk, Institute for Biological Sciences, National Research Council of Canada, Ottawa Ontario K1A 0R6, Canada; e-mail: wakarchu@biologysx.lan.nrc.ca.

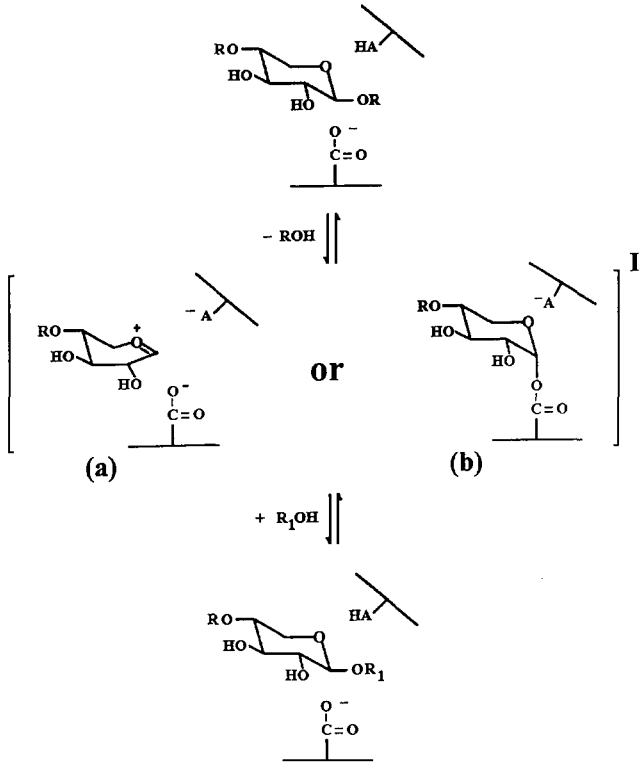

Fig. 1. General reaction mechanism for a retaining endo-β-D-xylanase. The structures of the substrate, intermediates, and product have been simplified for clarity. R = $xyl_{(n)}$, HA = the acid catalyst, I = the structures inside the brackets are possible intermediates, and R_1 = H or $xyl_{(n)}$. The reaction proceeds by a double displacement mechanism where general acid catalysis/nucleophilic attack on the anomeric center produces 1 of 2 possible intermediates. Intermediate (a) has a carboxylate acting in an ion pair to stabilize an oxo-carbonium ion, whereas intermediate (b) shows that the transition state has collapsed into a covalent glycosyl-enzyme. Either of these intermediates could then react with a nucleophilic water (R_1 = H) to produce hydrolysis products or another xylo-oligosaccharide (R_1 = $xyl_{(n)}$) to produce trans-glycosylation products. The transition states for both steps are likely to have substantial oxo-carbonium ion character.

sis, and that Tyr 69 and Tyr 80 are likely involved in substrate binding.

Results

Mutagenesis of conserved amino acid residues

Prior to the solution of the structure of the *B. circulans* xylanase by crystallography, we had used site-directed mutagenesis to examine several acidic amino acid residues that are conserved in the family G xylanases (Fig. 2). Two glutamic acid residues, Glu 78 and Glu 172 (numbering refers to the position in the *B. circulans* sequence), are absolutely conserved, along with 1 additional acidic residue, Asp 83, which is an aspartic acid in the bacterial xylanase sequences and a glutamic acid in the fungal xylanase sequences. Originally, 2 other aspartic acid residues were also targeted for mutagenesis on the basis of their sequence conservation in this family. However, there are now members known in this family that lack these aspartic acid residues, and their overall conservation is 11 of 15 for Asp 11 and 13 of 15 for Asp 106 in these sequences. Once the crystal structure of the *B. circulans* enzyme was known, the absolutely conserved glutamic acid residues were observed in the active site cleft (Campbell et al., 1993).

The specific activities of the acidic residue mutants show that only mutations at Asp 11, Glu 78, and Glu 172 have a significant effect on catalysis (Table 1). The retention of enzyme activity in the D11N mutant shows the acidic side chain of Asp 11 is not essential for catalysis in this enzyme. When the glutamic acid residues are mutated to glutamine (E78Q and E172Q), no enzyme activity can be detected; however, when the carboxylate side chain is maintained but the side-chain length is shortened in E78D and E172D, some residual activity is observed (Table 1). The large decrease in activity seen with the mutant enzymes E78D and E172D, 0.04% and 0.16% residual activity respectively, strongly suggests that these are the catalytic amino acid residues. These residues correspond to the *B. pumilis* xylanase residues Glu 93 and Glu 182, which were shown to be important in that enzyme (Ko et al., 1992).

Table 1. *Enzymatic properties of various xylanase mutants*

Enzyme	Activity (% of wild type)	$K_{m(app)}$ (mg/mL)	$k_{cat(app)}$ (min^{-1})	$k_{cat(app)}/K_{m(app)}$ (min^{-1} mg^{-1})
BCX (wild type)	100	1.9 ± 0.2[a]	8,918	4,693
D11N	25	0.92 ± 0.02	2,245	2,440
E78D	0.043	2.3 ± 0.2	3.9	1.7
E78Q	<0.01[b]	nd[c]	nd	nd
E172D	0.19	4.4 ± 0.5	17.1	3.9
E172Q	<0.01	nd	nd	nd
E172C	<0.01	nd	nd	nd
Y69F	<0.01	nd	nd	nd
Y80F	0.045	12 ± 2	3.7	0.3
Y166F	76	1.2 ± 0.12	6,807	5,672
R112K	83	5.9 ± 0.4	7,373	1,249
R112N	35	5.5 ± 0.7	3,122	568

[a] The confidence levels are the averages of the standard deviation as calculated by Enzfitter.
[b] This is the detection limit of the assay.
[c] Not determined.

Fig. 2. Amino acid sequence alignment of low molecular mass xylanases. The sequence alignment is based on structural considerations, not simply on computer-generated alignments. The sequences of *Bacillus subtilis* and *Trichoderma viride* have been omitted because the *B. subtilis* sequence is identical to *Bacillus circulans* except at position 147, and *T. viride* is essentially identical to *Trichoderma reesei* except at positions 9, 143, 144 (Oku et al., 1993). The sequences are B. pum. = *Bacillus pumilis* (Fukasaki et al., 1984); C. aceto. = *Clostridium acetobutylicum* (Zappe et al., 1990); R. flav. = *Ruminococcus flavefaciens* (Zhang J, Flint HJ, 1992, EMBL Database accession #Z11127); T. ree. II = *T. reesi* XYN II (Torronen et al., 1992); T. harz. = *Trichoderma harzianum* (Yaguchi et al., 1992); S. comm. = *Schizophyllum commune* (Oku et al., 1993); S. sp 36a = *Streptomyces* sp. 36a (Nagashima et al., 1989); S. liv. B = *Streptomyces lividans* XYN B (Shareck et al., 1991); S. liv. C = *S. lividans* XYN C (Shareck et al., 1991); B. circ. = *B. circulans* (Yang et al., 1988); A. niger = *Aspergillus niger* (de Graaff et al., 1992); A. tubig = *Aspergillus tubigenesis* (Maat et al., 1992); T. ree. I = *T. reesei* XYN I (Torronen et al., 1992).

The solution of the high resolution X-ray crystal structure revealed a long, deep cleft formed at the intersection of 2 β-sheets and bordered by an extended, flexible loop (Kinemage 1). The conserved glutamic acid residues were found on either side of the cleft in positions similar to Glu 35 and Asp 52 of HEWL. In addition to the conserved acidic residues, there are a number of other conserved residues that the crystal structure shows are in the active site cleft (Fig. 3). We targeted Tyr 69, Tyr 80, Tyr 166, and Arg 112 to investigate the role that these residues may play in the reaction mechanism. Mutation of the conserved Tyr 80 to phenylalanine (Y80F) resulted in a dramatic loss of activity, leaving only 0.03% residual activity (Table 1), whereas the mutation Y69F resulted in a total loss of detectable enzyme activity. In contrast to these other tyrosine mutants, the mutation Y166F has only a minor effect on enzyme function. The Tyr 166 residue is not absolutely conserved in this enzyme family (Fig. 2), and consequently the contribution of the hydroxyl group may not be that important. Mutation of the conserved Arg 112 to lysine (R112K) also resulted in no change in the enzyme activity, but conversion to asparagine (R112N) resulted in a 68% drop in specific activity. Those mutants showing a decreased but measurable enzymatic activity were examined further for their kinetic properties.

Kinetic analyses of the active site mutants

The kinetic analysis of xylanases is hampered by the lack of a suitable synthetic substrate for colorimetric measurements. Therefore the analysis of the active site mutants had to be performed using a reducing sugar assay to measure hydrolysis of a soluble xylan preparation. There has been much discussion in the literature about the merits of various reducing sugar assays, but we chose to use the assay reagent described by Lever (1972). This assay has very sensitive detection limits (μM) and is insensitive to the chain length of the released oligosaccharides (data not shown), which allows a more accurate estimation of the newly generated reducing ends. The major limitation of the assay method is that the inhomogeneous substrate changes during the reaction ($K_{m(app)}$ increases with time, data not shown), so particular care was taken to ensure that the extent of hydro-

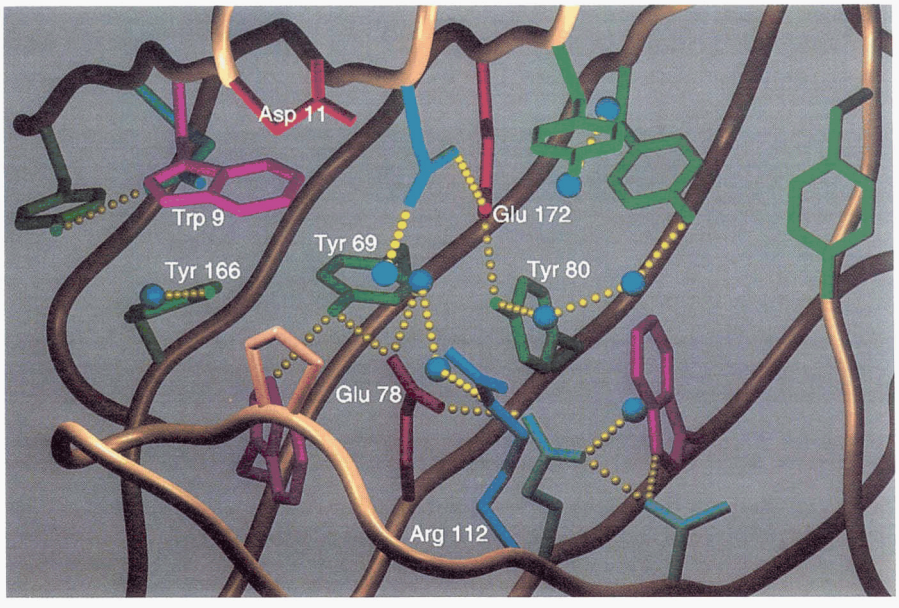

Fig. 3. The active site cleft of the *B. circulans* xylanase. The structure of the enzyme has been presented here with the molecular graphics program SETOR (Evans, 1993), with the carbon backbone shown as a gold tube and selected side chains displayed within the active site cleft. The residues are colored according to residue type, with Glu and Asp in red, Tyr in green, Trp in magenta, Arg in blue and Gln and Asn in cyan. Potential hydrogen bonds were calculated using the default criteria in the program QUANTA (Molecular Simulations, Inc.) and are shown here as the yellow dotted lines. The blue spheres are water molecules.

lysis was the same for each enzyme examined, such that a relative comparison of kinetic parameters would be possible.

Despite the limitation of our reducing sugar assay, it was sensitive enough to allow analysis of the E78D, E172D, and Y80F mutant proteins, which had very low levels of enzyme activity (Table 1). There was only a minor increase in the $K_{m(app)}$ for the E172D enzyme and no change in the $K_{m(app)}$ for the E78D enzyme. This indicates that the active site structure of the enzyme must be maintained in these mutants and that the major effect of these mutations is on catalysis rather than substrate binding. In contrast to the other mutants, the Y80F enzyme showed a moderate increase in the $K_{m(app)}$ for the soluble xylan substrate and a large decrease in catalytic activity.

Withers et al. (1992) have shown that 2 of their β-glucosidase active site mutants, E358N and E358Q, had small amounts of contaminating activity that could be attributed to either the corresponding Asp mutant or wild type. We considered the possibility that the low level of activity observed in some mutants was from a small amount of contaminating wild-type enzyme produced by translational misreading in *Escherichia coli* or spontaneous deamidation of the amide mutants; however, we never observed residual activity in enzyme preparations from the mutants E78Q, E172Q, E172C, and Y69F. Also in the case of the Y80F mutant, the $K_{m(app)}$ is significantly higher than the wild type. Therefore, we believe that the observed activity is from the mutant proteins.

CD spectra of the active site mutants

To insure the mutant proteins were not improperly folded, we analyzed the active site mutants by CD spectroscopy. The spectra are basically unremarkable, with the E78D and Y80F mutants showing a slight deepening of the trough at 220 nm (Fig. 4). All of the other mutants analyzed show spectra that overlap with the wild type. These data suggest that the reduced activity of these mutants as well as the inactive mutants (e.g., Y69F) is not due to any gross alterations in the structure.

Structure of an enzyme–substrate complex

The solution of the high resolution X-ray crystal structure of the *B. circulans* xylanase allowed identification of the conserved residues in the active site of the enzyme (Fig. 3; Kinemage 2; Campbell et al., 1993). The presence of several tyrosines in the cleft suggests likely sites for the formation of hydrogen bonds to the substrate. It was, however, not obvious how the substrate would

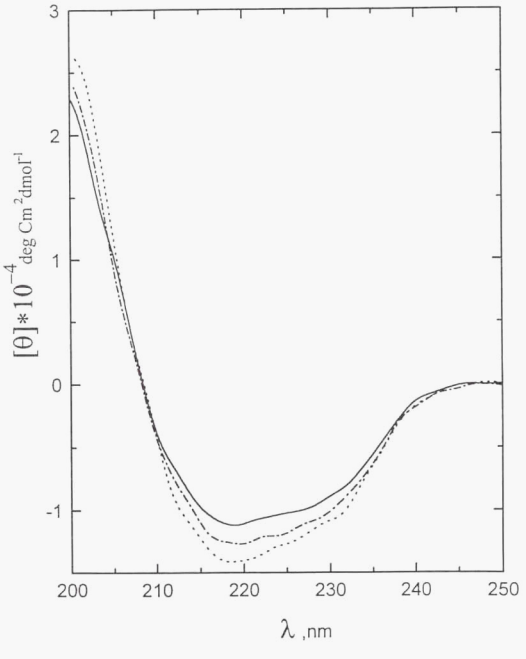

Fig. 4. CD spectra of selected active site mutants of the *B. circulans* xylanase. The wild-type enzyme spectrum is shown by the solid line, the E78D mutant spectrum is shown by the - - - - line, and the Y80F spectrum is shown by the mixed —·—·— line.

fit into the cleft of the enzyme. We attempted to produce co-crystals of the enzyme and small xylo-oligosaccharide substrates using the catalytically incompetent mutant E78Q, without success. Previously we had prepared several single cysteine mutants for making heavy atom derivatives for crystallography. One of those, E172C, was not enzymatically active (Table 1) and we succeeded in producing co-crystals of this mutant with xylotetraose.

The structure of the enzyme is essentially unchanged upon binding the substrate. The 2 structures superimpose with an RMS deviation of 0.137 Å for all main-chain atoms. The flexible loop (residues 111–131) moves only a small amount, opening the cleft to accommodate the substrate. The Cα atoms of residues 118–120 shift by between 0.6 and 0.7 Å. The only other changes in the protein are at the site of the mutation and a rotation of the side chain of Asn 35, which forms a hydrogen bond to Glu 172 in the native structure.

Only 2 xylose residues could be fitted into the electron density, suggesting that either the enzyme has a very small amount of residual activity in the crystal or that the enzyme requires a larger substrate for tight binding. The electron density that is observed for the substrate is weaker than for the nearby protein atoms including the flexible loop region, suggesting that the substrate is bound at less than 100% occupancy. The structure was initially refined with the occupancy set to 100% and the average *B*-factor was found to be 26 Å^2 for the substrate, whereas the average *B*-factor for the main-chain atoms of the loop region was 16 Å^2. Refinement of the *B*-factors with the occupancy set to 70% resulted in the average *B*-factor for the substrate of 16 Å^2. When the difference electron density map was contoured at a high level (4σ), density was observed primarily at the positions of the oxygen atoms (data not shown), thus unambiguously demonstrating the direction of the carbohydrate chain. The refined xylobiose structure had ϕ and ψ angles of 120° and 163°, respectively, similar to the ideal geometry of 175° and 135°, respectively. When the difference electron density map was contoured at 2.5σ, a small tail of density was seen extending beyond the O4 oxygen at the nonreducing end of the first visible xylose residue (Fig. 5). This suggests that the rest of the substrate extends beyond the active site cleft and is too mobile to be seen in the electron density.

The structure of this complex revealed some of the enzyme-substrate interactions (Fig. 6; Kinemages 2, 3). A stacking interaction of Trp 9 with one of the xylose rings is evident as are hydrogen bonds between the 2 xylose rings and Tyr 69, Tyr 166, Arg 112, and the backbone carbonyl of Pro 116 (Table 2). The terminal oxygen of the reducing end of the xylotetraose is in close proximity to the 2 glutamic acid residues.

Table 2. *Summary of close contacts between B. circulans xylanase and the substrate xylotetraose*

Substrate ring	Substrate atom	Protein atom	Distance (Å)
Xyl 1	O3	OH Tyr 166	2.82
	O2	OH Tyr 69	2.88
	C5	CE2 Trp 9	3.37
	C5	NE1 Trp 9	3.10
Xyl 2	C1	OE1 Glu 78	3.37
	O1	OE1 Glu 172[a]	2.15
	O2	OE2 Glu 78	3.00
	C1	OH Tyr 80	3.57
	O2	NE Arg 112	2.97
	O3	NH2 Arg 112	3.15
	O3	O Pro 116	2.56

[a] Position of Glu 172 is taken from the native structure after superimposition onto the complex structure.

Discussion

The reaction mechanism of retaining β-glycosidases has been examined for many years, and it was first determined in HEWL that 2 acidic residues were involved in catalysis (Blake et al., 1967; Phillips, 1967). Several other glycosidases have now been examined and the lysozyme paradigm for acid catalysis has been a common theme among them (Sinnott, 1990; Mooser, 1992). An extension of these earlier observations is possible when one can assign a role for a specific residue within the active site. Considering the proposed mechanism for retaining glycosidases, it is important to determine which residue is the nucleophile (or charge-stabilizing residue) and which is the acid-base catalyst. The nucleophile involved in a β-glucosidase, a β-galactosidase,

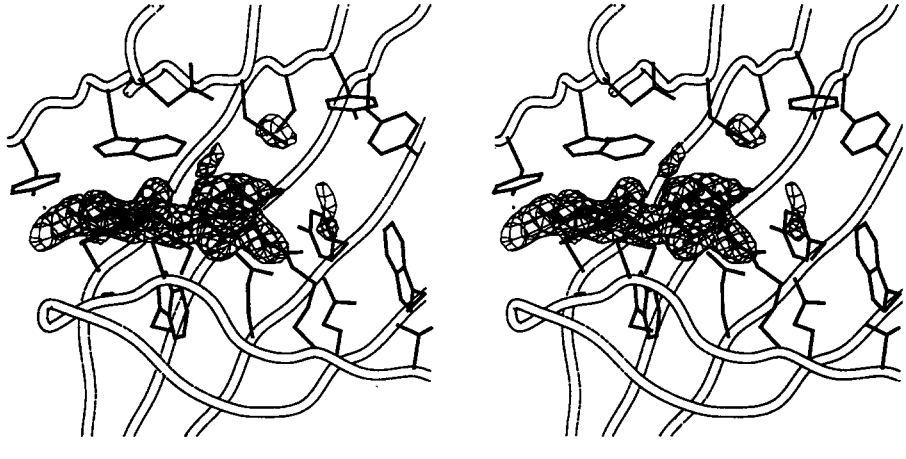

Fig. 5. Stereo diagram of the $F_o - F_c$ difference map for the E172C-xylotetraose complex. The phases were calculated from the refined structure and F_c was calculated after omitting the substrate and all of the water molecules.

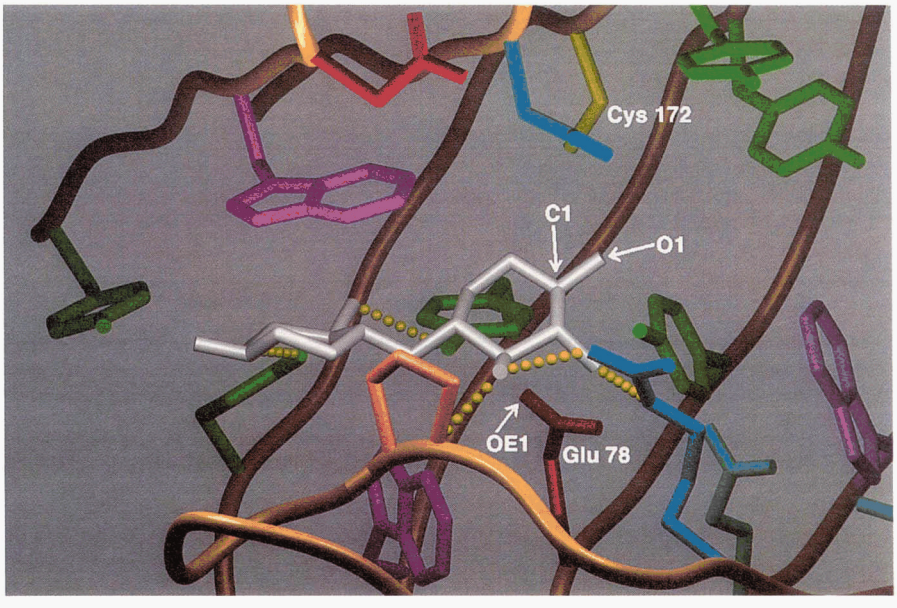

Fig. 6. View of the *B. circulans* xylanase active site for the mutant E172C, in complex with xylotetraose. This representation is similar to that shown in Figure 2, except that Cys 172 is shown in gold, and some residue labels have been omitted for clarity. Atoms C1 and O1 of the second xylose residue are indicated. Only potential hydrogen bonds to the substrate have been shown.

a cellobiohydrolase, and an endoglucanase have been trapped through the use of suicide inhibitors (Withers & Street, 1988; Gebler et al., 1991; Tull et al., 1991; Wang et al., 1993). The only published high resolution structures for retaining endo-β-glycosidases are lysozymes. The crystallographic assignment of Asp 52 as the charge-stabilizing residue in HEWL comes from the early work of Blake et al. (1967) and from the more recent examination of the structure by Strynadka and James (1991). The Asp 20 residue in T4 phage lysozyme is thought to play a similar role to Asp 52 in HEWL (Anderson et al., 1981). In our enzyme–substrate complex, the orientation of the substrate suggests that Glu 78 and Glu 172 would be in position to act as the nucleophile and the acid–base catalyst, respectively. The distance from the OE1 atom of E78 to the C1 atom of the reducing end of the xylotetraose (Fig. 6; Table 2) is similar to the distance from OD2 of Asp 52 to C1 of the saccharide in subsite D from a trisaccharide complex with HEWL (Strynadka & James, 1991). Supporting evidence for the role of Glu 78 as the nucleophile is the proximity of Arg 112 to Glu 78. Although no salt link is found in this structure, unlike the situation in the *B. pumilis* xylanase (Katsube et al., 1990), the presence of a positive charge in the vicinity may help to lower the pK_a of Glu 78, thus maintaining it in a negatively charged state. In addition, mutational analysis shows that enzyme activity is more affected in the E78D mutant than in the E172D mutant, which is consistent with E78 having the more critical role of the nucleophile.

The Glu 172 position relative to the xylotetraose can be calculated by superimposition of the native structure onto that of the complex (Table 2). From this structure it can be seen that the positioning of Glu 172 relative to the hydroxyl group at C1 (O1) of xyl 2 is similar to that of Glu 35 in HEWL relative to the hydroxyl group at C1 of the NAM-NAG-NAM substrate (Strynadka & James, 1991). The distance between OE2 of Glu 172 and O1 of xyl 2 is shorter than a normal hydrogen bond. Therefore, in order to fit this substrate into the cleft of the native enzyme, further movement of the flexible loop would be required. Attempts to model substrates into the active site were prevented by steric hindrance with residues in the flexible loop (data not shown). Glutamic acid residues 78 and 172 are exposed to solvent to the same degree and both side-chain oxygens of each are within hydrogen bonding distance of other residues in the active site. In the native enzyme structure Glu 78 is hydrogen bonded to Gln 127 and Tyr 69, whereas Glu 172 is hydrogen bonded to Asn 35 and Tyr 80 (Fig. 3). It should be noted that this structure represents only a partial view of the enzyme–substrate interactions. A larger substrate spanning the whole active site may bind in a slightly different conformation likely with an accompanying change in the position of the loop. This would change the distances from the potential nucleophile and acid–base catalyst to the saccharide.

The structures of several carbohydrate-binding proteins and glycosidases have been determined (Rouvinen et al., 1990; Vyas, 1991; Juy et al., 1992; Mooser, 1992; Davies et al., 1993; Keitel et al., 1993). There are many features of carbohydrate-binding proteins and glycosidases that are similar, though the structures of these binding sites or active sites are quite different. The most striking similarity is the large number of aromatic residues, mainly tyrosine and tryptophan, which comprise the binding or active sites. The *B. circulans* active site contains 6 tyrosine and 3 tryptophan residues. The stacking interaction of Trp 9 with the face of a xylose ring is similar to a predicted stacking interaction of Trp 457, with a glucose residue at subsite D in the CelD active site (Juy et al., 1992), and also similar to the observed stacking interactions of Trp 135 with the face of a glucose residue in subsite A and that of Trp 367 with the face of a glucose residue in subsite C of the CBHII active site (Rouvinen et al., 1990). HEWL was the first retaining glycosidase for which this kind of aromatic stacking interaction with a sugar face was seen in the crystallographically determined protein structure (Phillips, 1967). There is a stacking interaction between Trp 62 and the nonpolar face of the *N*-acetylmuramic acid ring in subsite B (Strynadka & James, 1991). This stacking interaction appears to be a very common binding interaction in glycosidases.

The role of the tyrosines in the active site of *B. circulans* xylanase is less certain than the role played by the Trp 9 residue. Tyrosine residues have been implicated in the catalytic mecha-

nism for both the *E. coli* β-galactosidase (Mooser, 1992) and the *Agrobacterium faecalis* β-glucosidase (Withers, pers. comm.). In both cases the mutation of a single tyrosine to phenylalanine resulted in a dramatic decrease in activity. In the case of the *E. coli* β-galactosidase, it is hypothesized that Tyr 503 may be the proton donor in the reaction. In the β-glucosidase it is possible that Tyr 298 has a hydrogen bonding role with the C2-hydroxyl of the substrate. In the structure of the *B. circulans* xylanase complexed with xylotetraose, hydroxyl groups of the xylose rings are close enough to form hydrogen bonds with the hydroxyl groups of Tyr 69 and Tyr 166 (Table 2). Why then does the mutation Y69F completely inactivate the protein, whereas the mutant Y166F has only a negligible effect on enzyme activity? From the structure of the complex it can be calculated that Tyr 69 makes 2 hydrogen bonds, one with the C2 OH group of the nonreducing (second) xylose ring, and the second with the OE1 atom of Glu 78. This hydrogen bond to Glu 78 may help orient the nucleophile for the reaction, whereas the second helps to position the substrate. For enzyme activity then, the single hydrogen bond from Tyr 166 to the C3 OH of the second xylose ring appears to be less important for the reaction than those from Tyr 69.

Kinetic analysis of the Y80F mutant enzyme suggests a role for Tyr 80 in substrate binding. The closest atom of xyl 2 to the hydroxyl of Tyr 80 is C1 (Table 2; Fig. 6). This distance is slightly longer than that for Glu 78 to C1, suggesting that Tyr 80 does not have a direct role in catalysis. The steric conflicts seen in modeling the substrate as discussed previously would imply that the Tyr 80–C1 distance must be even longer in the complex of the substrate with the wild-type enzyme. In a complex with a longer substrate, Tyr 80 may have a role in hydrogen bonding to the substrate. In the native structure it appears to make a hydrogen bond to Glu 172 and thus may have a role in positioning the proposed acid–base catalyst.

In summary then, it would appear that disruption of the hydrogen bonds from the active site tyrosine residues to the nucleophile are more detrimental to enzyme activity than disruption of the hydrogen bonds to either the acid catalyst or the substrate alone. Experiments to examine the substrate binding interactions of this enzyme further and to produce a better complex that may answer some of these questions are under way.

Materials and methods

Bacterial strains, growth conditions, and standard methods

The following standard laboratory strains of *E. coli* were used for the propagation of recombinant plasmids, and the production of recombinant gene products: MV1190: Δ(*lac-proAB*), *thi*, *supE*44, Δ(*sr*1-*recA*)306::Tn10(tet^r) [F′: *traD*36, *proAB*, *lacI*^{q} ΔM15]; RZ1032: HfrKL16 PO/45 [*lysA*(61–62)], *dut*1, *ung*1, *thi*1, *relA*1, *Zbd*-279::Tn10, *supE*44; BHM 71-18: Δ(*lac-proAB*), *thi*, *supE*44, [*mut*S::Tn10(tet^r)], [F′: *proAB*, *lacI*^{q} ΔM15]; HB101: *hsdS*20 (r− m−), *leu*, *supE*44, *ara*14, *galK*2, *lacY*1, *proA*2, *rpsL*20 (Str^r), *xyl*-5, *mtl*-5, *recA*13, *mcrB*.

The synthetic gene for the *B. circulans* protein has been described (Sung et al., 1993). The gene was transferred to the vector used in this work, pCWori+. This was obtained from Ms. Amy Roth of the University of Oregon and it is a 5-kb pBR322 derivative, containing the ampicillin resistance marker, the *lacI* gene, part of the *lacZ* structural gene, 2 copies of the synthetic TAC promoter, and 1 copy of the lacUV5 promoter; in addition it carries the M13 phage origin of replication, which confers the ability to produce single-stranded DNA (ssDNA) when cells containing it are superinfected with a helper phage. All liquid cultures were grown in either 2YT medium (16 g yeast extract, 10 g bacto-tryptone, 5 g NaCl, 1 L of H_2O), or TB medium (24 g yeast extract, 12 g bacto-tryptone, 10 mL 1 M potassium phosphate buffer, pH 7.5, 5 mL of 80% glycerol, 1 L H_2O). The antibiotic ampicillin was added at 150 mg/L to all cultures of plasmid-containing strains. The cultures were grown with shaking at 30 °C for protein and plasmid production, and at 37 °C for the production of ssDNA-containing particles.

Basic recombinant DNA methods such as plasmid DNA isolation, restriction enzyme digestions, the purification of DNA fragments for cloning, ligations, transformations, and DNA sequencing were performed as recommended by the enzyme supplier or the manufacturer of the kit used for the particular procedure. Restriction and DNA modification enzymes were purchased from New England Biolabs Ltd., Mississauga, Ontario. Prep-A-Gene DNA purification matrix was purchased from Bio-Rad laboratories, Mississauga, Ontario, Canada. Sequenase, DNA sequencing kit was purchased from US Biochemicals, Cleveland, Ohio. Oligonucleotide 3′ end labeling with digoxigenin–ddUTP and the subsequent chemiluminescent detection were performed with a kit and some additional reagents from Boehringer Mannheim Canada, Laval, Quebec. Protein concentration was determined from the molar extinction coefficient of the xylanase: 81,790 L mol^{-1}, $A_{280}^{0.1\%} = 4.08$; no correction was made for the Tyr to Phe mutations.

Site-directed mutagenesis

Mutagenesis was performed either using the UDNA method as described by Kunkel et al. (1987) or by constructing synthetic restriction fragment cassettes for replacement of specific regions of the gene (Sung et al., 1993). Oligonucleotides were synthesized using an Applied Biosystems model 380A DNA synthesizer, using the phosphoramidite method. Synthetic oligonucleotides were purified by polyacrylamide gel electrophoresis in 15% gels containing 7 M urea. The clones containing a functional xylanase gene were identified by screening transformants on plates containing remazol-brilliant blue xylan. Colonies that expressed the gene for an active xylanase were identified by the production of halos (Kluepfel, 1988). Inactive mutants were identified from colony hybridization reactions with the mutagenic oligonucleotide as a probe. Clones with a positive hybridization signal were sequenced and then repurified by transformation to ensure the purity of the clone. DNA sequencing was again performed to verify that there were no other changes other than at the desired codons.

Protein purification was performed as described previously (Sung et al., 1993), with the modification that the ion exchange column was a POROS HSII perfusion column (Perseptive Biosystems, Inc.).

Measurement of enzymatic activity

The activity of the enzyme was measured by the quantitative assay of the number of reducing sugar end groups generated from hydrolysis of soluble xylan. The substrate for this assay was the

fraction of birchwood xylan that dissolved in water from a 5% suspension of birchwood xylan (Sigma Chemical Company). After removing the insoluble fraction, the supernatant was freeze dried and stored in a desiccator.

The measurement of specific activity was performed as follows. Reaction mixtures contained 10 mg/mL xylan in assay buffer (20 mM MES-NaOH, 50 mM NaCl, pH 6.0), with enzyme suitably diluted in 1 mg/mL bovine serum albumin, in assay buffer. The substrate and buffer were mixed and prewarmed to 40 °C, and the reaction was started by the addition of the enzyme. At various time intervals 50-μL portions were removed and the reaction was stopped by dilution into 1 mL of 5 mM NaOH. The amount of reducing sugars was determined with the hydroxybenzoic acid hydrazide reagent (Lever, 1972). A unit of enzyme activity was defined as that amount generating 1 μmol reducing sugar in 1 min at 40 °C, using xylose as a standard.

For the determination of kinetic parameters, substrate concentrations from 0.4 mg/mL to 20 mg/mL were used. The time used for the enzyme reactions was 5 min, using a final protein concentration of 300 ng/mL for the wild type. Mutant proteins were used at concentrations that gave the same overall hydrolysis level as the wild-type control. Kinetic parameters were calculated using the computer program Enzfitter (Leatherbarrow, 1987).

CD spectroscopy

The CD spectra of the xylanase proteins was obtained from a JASCO J-600 spectropolarimeter. The instrument was calibrated with ammonium-*d*-camphorsulfonate. Spectra in the far UV region (200–250 nm) were measured in a 0.02-cm-pathlength cylindrical quartz cell at a protein concentration of 0.5 mg/mL.

X-ray crystallography

Crystals of the complex of the *B. circulans* xylanase mutant E172C and xylotetraose were grown by the hanging drop vapor diffusion method. The reservoir buffer was 40 mM Tris, pH 7.5, 22% saturated $(NH_4)_2SO_4$, and 100 mM NaCl. The initial protein concentration in the droplet was about 4 mg/mL after adding an equal volume of reservoir solution to the protein solution with a 10-fold molar excess of xylotetraose. Droplets were seeded after 1 day of equilibration. The space group of the crystals was $P2_12_12_1$ with $a = 44.00$ Å, $b = 52.78$ Å, and $c = 78.39$ Å. The X-ray diffraction data were collected on a San Diego Multiwire Area Detector system on a Rigaku rotating anode generator. All data reduction was performed using the San Diego software and the PHASES program package (Furey & Swaminathan, 1990). The initial electron density map was calculated with phases from the native protein structure (Campbell et al., 1993), which has been refined to an R-factor of 0.165 for data between 8 and 1.49 Å resolution. The starting conformation of the xylotetraose substrate was an idealized structure provided by Dr. David Bundle. The values for the torsion angles, ϕ (measured from atoms C2-C1-O4-C4) and ψ (C1-O4-C4-C3) were 175° and 135°, respectively, in the ideal model. The substrate was built into the difference electron density with O (Jones et al., 1990) and the complete structure (with the occupancy of the substrate maintained at 100%) was refined using the simulated annealing and minimization protocols of X-PLOR (Brünger, 1988). The final model contains 1,445 non-hydrogen protein atoms, 2 xylose residues, 1 sulfate molecule, and 144 water molecules. The resulting R-factor was 0.161 for data between 8 and 1.8 Å resolution with $F > 2\sigma(F)$. RMS deviations from ideality are 0.008 Å for bonds, 1.66° for angles, 27.28° for dihedrals, and 1.26° for impropers.

Acknowledgments

We acknowledge the expert technical assistance of Natalie Methot, Anna-Maria Valley, Rebbeca To, and David Watson. We also thank Drs. Martin Young, Lawrence McIntosh, and Steve Withers for critical reading of the manuscript. This work was performed as part of a project within the Protein Engineering Network of Centres of Excellence in Canada. This is NRCC publication number 37366.

References

Anderson WF, Grutter MG, Remington SJ, Weaver LH, Matthews BW. 1981. Crystallographic determination of the mode of binding of oligosaccharides to T4 bacteriophage lysozyme: Implications for the mechanism of catalysis. *J Mol Biol 147*:523–543.

Blake CCF, Johnson LN, Mair GA, North ACT, Phillips DC, Sarma VR. 1967. Crystallographic studies on the activity of hen egg-white lysozyme. *Proc R Soc Lond B 167*:365–377.

Bray MR, Clarke AJ. 1990. Essential carboxy groups in xylanase A. *Biochem J 270*:91–96.

Brünger AT. 1988. Crystallographic refinement by simulated annealing: Application to a 2.8 Å resolution structure of aspartate aminotransferase. *J Mol Biol 203*:803–816.

Campbell R, Rose D, Wakarchuk W, To R, Sung W, Yaguchi M. 1993. A comparison of the structures of the 20 kD xylanases from *Trichoderma harzianum* and *Bacillus circulans*. In: Suominen P, Reinikainen T, eds. *Proceedings of the second TRICEL symposium on Trichoderma reesei cellulases and other hydrolases, Espoo, Finland, 1993*. Helsinki: Foundation for Biotechnical and Industrial Fermentation Research. pp 63–72.

Chauvaux S, Beguin P, Aubert JP. 1992. Site-directed mutagenesis of essential carboxylic residues in *Clostridium thermocellum* endoglucanase celD. *J Biol Chem 267*(7):4472–4478.

Davies GJ, Dodson GG, Hubbard RE, Tolley SP, Dauter Z, Wilson KS, Hjort C, Mikkelsen JM, Rasmussen G, Schulein M. 1993. Structure and function of endoglucanase V. *Nature 365*:362–364.

de Graaff LH, van den Broeck HC, van Ooijen AJJ, Visser J. 1992. Structure and regulation of an *Aspergillus* xylanase gene. In: Visser J et al., eds. *Xylan and xylanases*. Amsterdam: Elsevier Science B.V. pp 235–246.

Evans S. 1993. SETOR: Hardware lighted three-dimensional solid model representations of macromolecules. *J Mol Graphics 11*:134–138.

Fukasaki E, Panbangred W, Shinmyo A, Okada H. 1984. The complete nucleotide sequence of the xylanase gene (XynA) of *Bacillus pumilis*. *FEBS Lett 171*:197–201.

Furey W, Swaminathan S. 1990. PHASES—A program package for the processing and analysis of diffraction data from macromolecules. *Proc American Crystallographic Association Meeting, New Orleans, Louisiana*. p 73.

Gebler JC, Aebersold R, Withers SG. 1991. Glu 537, not Glu 461 is the nucleophile in the active site of (lacZ) β-galactosidase from *Escherichia coli*. *J Biol Chem 267*:11126–11131.

Gebler J, Gilkes NR, Claeyssens M, Wilson DB, Béquin P, Wakarchuk WW, Kilburn DG, Miller RC, Warren RAJ, Withers SG. 1992. Stereoselective hydrolysis catalyzed by related β-1, 4-glucanases and β-1, 4-xylanases. *J Biol Chem 267*:12559–12561.

Gilbert H, Hazlewood G. 1993. Bacterial cellulases and xylanases. *J Gen Microbiol 139*:187–194.

Gilkes NR, Henrissat B, Kilburn DG, Miller RC Jr, Warren RAJ. 1991. Domains in microbial β-1,4-glycanases: Sequence conservation, function, and enzyme families. *Microbiol Rev 55*:303–315.

Jones TA, Bergdoll M, Kjeldgaard M. 1990. O: A macromolecular modeling environment. In: Bugg CE, Ealick SE, eds. *Crystallographic and modeling methods in molecular design*. New York: Springer-Verlag. pp 63–72.

Juy M, Amit AG, Alazri PM, Poljak RJ, Claeyssens M, Beguin P, Aubert JP. 1992. Three-dimensional structure of a thermostable cellulase. *Nature 357*:89–91.

Katsube Y, Hata Y, Yamaguchi H, Moriyama H, Shinmyo A, Okada H. 1990. Estimation of xylanase active site from crystalline structure. In: Ikehara M, ed. *Protein engineering: Protein design in basic research, medicine and industry*. Tokyo: Japan Scientific Societies Press. pp 91–96.

Keitel T, Simon O, Boriss R, Heinemann U. 1993. Molecular and active-site structure of a *Bacillus* 1,3-1,4-β-glucanase. *Proc Natl Acad Sci USA 90*:5287–5291.

Kempton JB, Withers SG. 1992. Mechanism of *Agrobacterium* β-glucosidase: Kinetic studies. *Biochemistry 31* (41):9961–9969.

Kluepfel D. 1988. Screening of prokaryotes for cellulose and hemicellulose degrading enzymes. *Methods Enzymol 160*:180–186.

Ko EP, Akatsuka H, Moriyama H, Shinmyo A, Hata Y, Katsube Y, Urabe I, Okada H. 1992. Site-directed mutagenesis at aspartate and glutamate residues of xylanase from *Bacillus pumilus*. *Biochem J 288*:117–121.

Kunkel TA, Roberts JD, Zakour RA. 1987. Rapid and efficient site-specific mutagenesis without phenotypic selection. *Methods Enzymol 154*:367–382.

Leatherbarrow RJ. 1987. *Enzfitter, a non-linear regression data analysis program for the IBM-PC*. Amsterdam: Elsevier Science Publishers B.V.

Lever M. 1972. A new reaction for colorimetric determination of carbohydrates. *Anal Biochem 47*:273–279.

Maat J, Roza M, Verbakel J, Stam H, Santos da Silva M, Bosse M, Egmond M, Hagemanns M, Gordcom R, Hessing J, Hondel C, Rotterdam C. 1992. Xylanases and their application in bakery. In: Visser J et al., eds. *Xylan and xylanases*. Amsterdam: Elsevier Science B.V. pp 349–360.

Mooser G. 1992. Glycosidases and glycosyltransferases. In: Sigman DS, ed. *The enzymes, vol XX*. pp 187–233.

Nagashima M, Okumoto Y, Okanishi M. 1989. Nucleotide sequence of the gene of the extracellular xylanase in *Streptomyces* sp. No. 36a. *Trends Actinomycetologia 80*:91–96.

Oku T, Roy C, Watson D, Wakarchuk W, Campbell R, Yaguchi M, Jurasek L, Paice M. 1993. Amino acid sequence and thermostability of xylanase A from *Schizophyllum commune*. *FEBS 334*:296–300.

Paice MG, Gurnagul N, Page DH, Jurasek L. 1992. Mechanism of hemicellulose-directed prebleaching of kraft pulp. *Enzyme Microb Technol 14*:272–276.

Phillips DC. 1967. The hen egg white lysozyme molecule. *Proc Natl Acad Sci USA 57*:484–495.

Rouvinen J, Bergfors T, Teeri T, Knowles JKC, Jones TA. 1990. Three dimensional structure of cellobiohydrolase II from *Trichoderma reesei*. *Science 249*:380–386.

Shareck F, Roy C, Yaguchi M, Morosoli R, Kluepfel D. 1991. Sequences of three genes specifying xylanases in *Streptomyces lividans*. *Gene 107*:75–82.

Sinnott ML. 1990. Catalytic mechanisms of enzymic glycosyl transfer. *Chem Rev 90*:1171–1202.

Strynadka NCJ, James MNG. 1991. Lysozyme revisited: Crystallographic evidence for distortion of an *N*-acetylmuramic acid residue bound in site D. *J Mol Biol 220*:401–424.

Sung WL, Luk CK, Zahab DM, Wakarchuk W. 1993. Overexpression and purification of the *Bacillus subtilis* and *Bacillus circulans* xylanases in *Escherichia coli*. *Protein Express Purif 4*:200–216.

Torronen A, Mach RL, Messner R, Gonzalez R, Kalkkinen N, Harkki A, Kubicek C. 1992. The two major xylanases from *Trichoderma reesei*: Characterization of both enzymes and genes. *BioTechnology 10*:1461–1465.

Tull D, Withers SG, Gilkes NR, Kilburn DG, Warren RAJ, Aebersold R. 1991. Glutamic acid 274 is the nucleophile in the active site of a retaining exoglucanase from *Cellulomonas fimi*. *J Biol Chem 266*:15261–15265.

Viikari L, Ranua M, Kantelinen A, Sundquist J, Linko M. 1986. Bleaching with enzymes. *Proc Third International Conference on Biotechnology in the Pulp and Paper Industry, Stockholm*. pp 67–69.

Vyas NK. 1991. Atomic features of protein–carbohydrate interactions. *Curr Opin Struct Biol 1*:732–740.

Wakarchuk W, Methot N, Lanthier P, Sung W, Seligy V, Yaguchi M, To R, Campbell R, Rose D. 1992. The 20 kd xylanase of *Bacillus subtilis*: A structure/function analysis. In: Visser J et al., eds. *Xylan and xylanases*. Amsterdam: Elsevier Science B.V. pp 439–442.

Wang Q, Tull D, Meinke A, Gilkes NR, Warren RAJ, Aebersold R, Withers SG. 1993. Glu 280 is the nucleophile in the active site of *Clostridium thermocellum* CelC, a family A endo-β-1,4-glucanase. *J Biol Chem 268*:14096–14102.

Withers SG, Rupitz K, Trimbur D, Warren RAJ. 1992. Mechanistic consequences of mutation of the active site nucleophile Glu 358 in *Agrobacterium* β-glucosidase. *Biochemistry 31*:9979–9985.

Withers SG, Street IP. 1988. Identification of a covalent α-D-glucopyranosyl enzyme intermediate formed on a β-glucosidase. *J Am Chem Soc 110*: 8551–8553.

Yaguchi M, Roy C, Watson DC, Rollin F, Tan LUL, Senior DJ, Saddler JN. 1992. The amino acid sequence of the 20 kd xylanase from *Trichoderma harzianum* E58. In: Visser J et al., eds. *Xylan and xylanases*. Amsterdam: Elsevier Science B.V. pp 435–438.

Yang JL, Lou G, Eriksson KEL. 1992. The impact of xylanase on bleaching of kraft pulps. *TAPPI 75*:95–101.

Yang RCA, Mackenzie CR, Narang SA. 1988. Nucleotide sequence of a *Bacillus circulans* xylanase gene. *Nucleic Acids Res 16*:7187.

Zappe H, Jones WA, Woods DR. 1990. Nucleotide sequence of a *Clostridium acetobutylicum* P262 xylanase gene (xynB). *Nucleic Acids Res 18*:2179.